Chitosan-crosslinked polyvinyl alcohol anti-swelling hydrogel designed to prevent abdominal wall adhesion

Yiqiao Huang [a,1], Jiefang Zheng [a,1], Guohao Zeng [a,1], Huanhuan Xu [b], Yangyang Lv [b], Xue Liang [a], Lin Jin [a,b,*], Xianhan Jiang [a,**]

[a] *The Fifth Affiliated Hospital of Guangzhou Medical University, Guangzhou Medical University, Guangzhou, 510700, China*
[b] *International Joint Research Laboratory for Biomedical Nanomaterials of Henan, Zhoukou Normal University, Zhoukou, 466001, China*

ARTICLE INFO

ABSTRACT

Abdominal adhesion is a frequent clinical issue with a high incidence rate and consequences following intra-abdominal surgery. Although many anti-adhesion materials have been used in surgical procedures, additional research is still needed to determine which ones have the most robust wet tissue adhesion, the best anti-postoperative adhesion, and the best anti-inflammatory properties. We have developed an excellent tissue adhesion and anti-swelling polyvinyl alcohol-chitosan hydrogel (AS hydrogel). According to *in vitro* cell testing, AS hydrogel significantly decreased inflammation around cells and exhibited good biocompatibility. Further, we assessed how well AS hydrogel prevented intraperitoneal adhesion using a rabbit model with cecum and abdominal wall injuries. According to the data, AS hydrogel has excellent anti-inflammatory and biodegradability properties compared to the control group. It can also prevent intestinal and abdominal wall injuries from occurring during surgery. Based on these results, hydrogel appears to be a perfect new material to prevent postoperative abdominal wall adhesion.

1. Introduction

Postoperative tissue adhesions are a common occurrence in open and laparoscopic surgeries, which are a significant clinical complication in abdominal and pelvic surgery [1–4]. According to statistics, they have an incidence rate as high as 90 % [5]. Wound clots, mesothelial injuries, or foreign objects such as gauze are the leading causes of postoperative adhesions and abnormal fibrous connections between organs and surrounding tissues [6–10]. Almost every region of the body can develop postoperative adhesions, which can result in complications such as intestinal obstruction, reduced ventricular contractions, chronic pain, and female infertility [11–13]. As a result, patients may have lifetime risks, and their medical burden would significantly increase. Clinical adhesions are frequently relieved, and the signs and consequences of complications are alleviated with the application of adhesiolysis [14,15]. The incidence of adhesive recombination (approximately 80 %) can easily result in secondary injury to patients and additional medical risks, such as iatrogenic bleeding, so this method is still unable to significantly reduce it due to the possibility of new trauma caused by surgical release [16–18].

As a result, the development of novel, user-friendly anti-adhesion barriers has gained significance in clinical settings. Currently, commercial anti-adhesion materials are generally applied as solid films or powders, creating a sol-gel-like barrier on the surface of tissues as a physical barrier between injured tissues and adjacent organs [19–21]. However, these obstacles have little clinical efficacy due to defects, including poor tissue adhesion, fast degradation rate, and poor bodily retention. Simultaneously, the first week following surgery is crucial for a successful intervention time window and effective clinical adhesion prevention [22–24]. Thus, the key to effectively intervening in tissue adhesion is to inhibit fibrin deposition and fibroblast adhesion at the injured site in the early and late stages [25–27].

Here, we have developed a polyvinyl alcohol (PVA)-chitosan (CS) hydrogel (AS hydrogel) (Fig. 1A) with good anti-inflammatory properties and wet tissue adhesion property, which can be transported to the surgery or injured site through an endoscope or injection pipeline in

---

minimally invasive surgery to exert anti-inflammatory and anti-adhesion properties (Fig. 1B). This is done to improve the retention, adhesion, and anti-inflammatory capacity of the barrier in the body. Furthermore, this material has adjustable mechanical viscoelasticity, which allows it to adapt to physiological tissue movements such as bladder contraction and intestinal peristalsis.

2. Materials and methods

2.1. Materials and cell culture

CS was purchased from Yibei Co. (Jinan, Shandong), whereas PVA and ginpin were obtained from Maikeling Co. (Shanghai). Other chemicals were purchased from Guangzhou Chemical Reagent Co. (Guangzhou, Guangdong). The American Type Culture Collection provided the Human Proximal Tubular Epithelial Cells (HK2), Normal Intestinal Cells (HIEC-6)and Uroepithelial Cells (SV-HUC-1). The F–12K Medium (HyClone) was used to culture the SV-HUC-1 cell line. Conversely, 5 mM D-glucose (Gibco) was added to the minimum essential medium for the HK2 and HIEC-6 cell culture. The two cell lines were maintained in their respective basal media, to which 10 % fetal bovine serum (Gibco) and 1 % penicillin/streptomycin (Gibco) were added as supplements. The cells were incubated at 37 °C under 5 % carbon dioxide.

2.2. Fabrication and characterization of hydrogel

PVA (0.4 g) was dissolved in 10 mL of distilled water by heating and stirring at 100 °C for approximately 15–30 min, depending on the stirring speed, to create a 4 wt% PVA solution. After reaching room temperature, the solution was left to stand in the open. The PVA solution was then stirred with 0.5 g of water-soluble CS and agitated until a homogeneous mixture was obtained. To create chemical cross-linking between PVA and CS, 1 mL of 1 % genipin solution was added as a cross-linking agent, and the mixture was manually stirred for 3 min with a clean glass rod. The hydrogel was removed from the container, yielding a transparent AS hydrogel. The adhesion property was assessed by weight through tube interface stretching in air/water and adhesion on pig skin (water impact, torsion, and stretching) in water. The hydrogel morphology was examined using a scanning electron microscope (SEM). Furthermore, the evaluation of the swelling test involved soaking the hydrogel in water for varying durations of time.

2.3. Cell proliferation and cell counting assays

Cell viability was monitored using the MTS assay (G3580; Promega Corporation, Madison, WI). An AS hydrogel scaffold was pre-positioned in a set of six-well plates, where HK2 and SV-HUC-1 cells were grown at a density of 20,000 cells per well. Following an incubation period of 24, 48, and 72 h, we added an MTS solution and a standard culture medium to each well. The culture solutions were then aspirated using a pipette gun and transferred into a 96-well plate after these plates had been kept in an incubator for 2 h. The absorbance was then determined using an enzyme-labeled detector (Epoch2 microplate reader, BioTek) at a wavelength of 490 nm. We used the cell counting kit-8 (CCK-8)
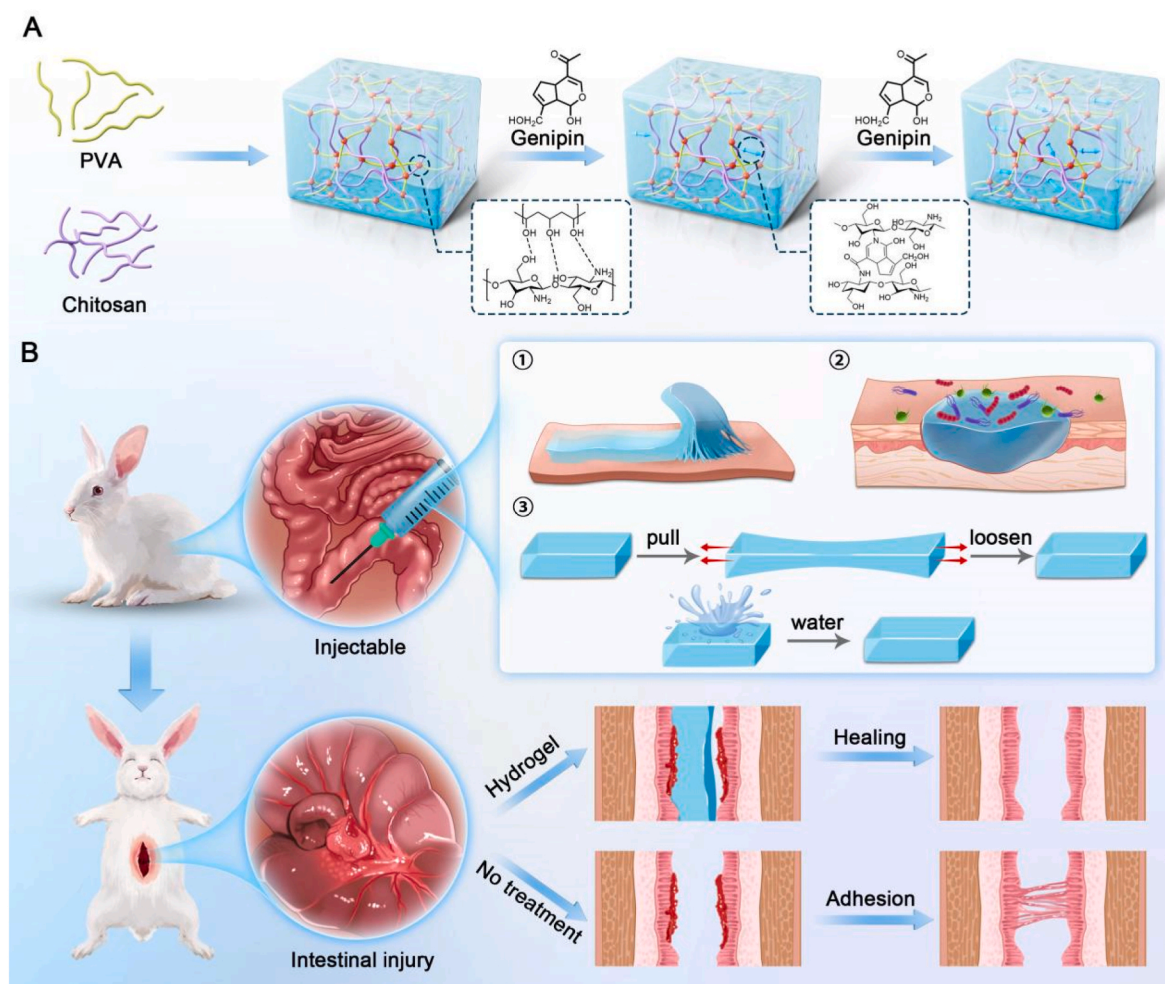

Fig. 1. Schematic of the AS hydrogel preparation and application. (A) AS hydrogel preparation, (B) wet tissue adhesion and anti-adhesion mechanism.

(Dojindo, Kumamoto, Japan) to detect cell proliferation. Following a similar approach, 96-well plates were seeded with HK2 and SV-HUC-1 cells at a concentration of 3×10^3 cells per well. A cultivation period of 24, 48, and 72 h was then observed. At these corresponding time intervals, we replaced the supernatant with a 10 % CCK-8 mixture volume (consisting of 10 μL CCK8 and 90 μL basal medium per well). Following a 2-h incubation period at 37 °C, the absorbances were measured at 450 nm using a microplate reader. Data obtained from the MTS and CCK-8 assays are presented as mean ± SEM values. Students' paired t-tests were used to identify statistically significant differences between the groups.

2.4. Live and dead cell double staining

In each well of a six-well plate, a blank control group and a PVA hydrogel group were set up. After UV disinfection, HIEC-6 cell line was seeded at a density of 2×10^5 cells per well for normal cultivation. Fluorescent staining was performed at 24 and 72 h using the Live and Dead Cell Double Staining Kit (Abbkine Co.). The kit includes solutions of Calcein-AM and propidium iodide (PI) for staining live and dead cells, respectively. After washing the cells with PBS and removing residual esterase activity, 100 μl of detection solution was added to the cells, and the mixture was incubated at 37 °C for 15 min. Fluorescence was detected using a fluorescence microscope with excitation at 490 nm to simultaneously monitor live and dead cells.

2.5. Cytoskeletal immunofluorescence

In a six-well plate with AS hydrogel matrix in each well, SV-HUC-1 cells or HK-2 cells were seeded. Approximately 2×10^5 cells were maintained per well as the cell density. We then incubated the plates for 8 h. Following incubation, 2 mL of 4 % paraformaldehyde was used to fix the cells for 20 min. Subsequently, the cell membranes were permeabilized with 2 mL of a 3 % Triton X-100 solution for 20 min. The cells were treated with a diluted 1:500 solution of either phalloidin-FITC or phalloidin-rhodamine (Sigma-Aldrich Co.). In a dark environment, the cells were incubated overnight. Finally, 200 μL of a blocking solution that contained 4′,6-diamidino-2-phenylindole for anti-fluorescence quenching was added to the cells. Confocal fluorescence microscopy was then used to identify the immunofluorescence signal at room temperature.

2.6. Cellular inflammatory factor assay

An experiment using SV-HUC-1 cells in co-culture was conducted using the AS hydrogel. The supernatant was collected and investigated further after the cell culture was incubated for 72 h at a constant temperature. A 12-cytokine combined detection kit (JS-SOP-001, Hangzhou Sage Bio) was then used to evaluate this supernatant. Specific reagents were added one at a time during the assay process, followed by a 2.5-h incubation at room temperature under light protection. After 5 min of centrifuging the samples at 200 g, the supernatant was discarded. Each sample tube was subjected to flow cytometry analysis after resuspension in 100 μL of phosphate-buffered saline (PBS). Data analysis involved constructing a standard curve to assist the quantification of the cytokines in the samples. The mean ± standard error of the mean (SEM) was used to present the data. Student's paired t-tests were used to assess the statistical significance between groups. $P < 0.05$ was considered statistically significant.

2.7. In vivo anti-adhesion evaluation of AS hydrogels

After a laparotomy, adult male rabbits of prominent New Zealand white breeds were selected for postoperative anti-adhesion experiments. A triple-blind method was used to model abdominal wall and cecum injuries in great white rabbits [28–30]. Three rabbits from the control

group and the AS hydrogel group comprised the two randomly selected groups from the experimental animals (n = 3). Blood samples were obtained prior to surgery to record inflammatory indicators. Following the intramuscular administration of anesthetics (ketamine 30 mg/kg + tamsulosin 50 mg/kg), the abdomens of the rabbits were exposed entirely for routine surgical disinfection. The abdominal cavity was exposed by making an incision along the midline of the abdominal wall. The cecum was rubbed with surgical toothed forceps and sterile brushes until a visible defect appeared on the surface [31,32]. After that, the injury was fixed and labeled with sutures. A saline solution was administered to the plasma membrane and colon to avoid drying out. Subsequently, a toothed pinch was used to scratch the abdominal wall, resulting in a deep muscular abdominal wall injury that was then fixed and labeled with sutures. While the hydrogel group evenly placed AS hydrogel over the cecum and abdominal wall injuries until the wound was fully covered, the control group was just rinsed with saline. Ultimately, the abdominal cavity was sealed via layer-by-layer closure of the abdominal incision. Every surgical procedure was carried out in aseptic conditions. To prevent postoperative infections, cefradine (300 mg/kg) was administered once daily for three days following the surgery in addition to routine analgesics and other symptomatic treatments. Blood was collected on the third postoperative day to monitor changes in inflammation and other relevant indicators. After euthanasia on the fourteenth day following the surgery, an overdose of pentobarbital was injected through the tail vein. The adhesion status of the cecum and the adjacent intestinal or abdominal wall was then observed, photographed, and scored during dissection. Adhesion scores are as follows [33,34]: score 0, no adhesion; score 1, one thin filmy adhesion; score 2, multiple thin adhesions; score 3, thick adhesion with focal point; score 4, thick adhesion with plantar attachment or multiple thick adhesions with focal point; score 5, very thick vascularized adhesion or multiple plantar adhesions. The scores were independently assessed using a double-masked process.

2.8. Histological examinations

Following the execution of the rabbits, the cecum, abdominal wall, and adherent tissues of each group were obtained, preserved with 4 % paraformaldehyde, and sectioned following paraffin embedding. After the sections were de-waxed, hydrated, and stained, pathological alterations in the cecum and abdominal wall, as well as variations in fibronectin expression following surgery, were observed using a hematoxylin-eosin kit and Masson kit (Solarbio, China). Masson trichrome positive (blue) area calculation: ImageJ software was used to determine the Masson trichrome positive area's ratio to the imaged tissue's total area [35,36].

2.9. Immunohistochemistry (IHC)

Sections of the intestinal and abdominal walls' paraffin-embedded tissues measuring 3 μm in thickness were prepared for IHC. The tissue sections were then heated to 60 °C and subjected to gradient hydration to de-wax. For 15 min, 0.3 % hydrogen peroxide inhibited endogenous peroxide activity. After submerging the sections in a boiling citrate antigen repair solution, they were autoclaved for 10 min under water. After allowing the repair solution to naturally cool to room temperature, 10 % normal goat serum was added to prevent non-specific binding for 30 min. The sections were then incubated overnight in a humidified room at 4 °C with the following primary antibodies. Secondary antibodies were applied to the sections and incubated for 1 h at room temperature. The color was developed with 3,3′-diaminobenzidine tetrachloride. Images were obtained using a confocal microscope. Using Image-Pro Plus 6.0, integrated optical density (IOD) measurements were performed on IHC images for quantitative analysis to calculate the average optical density (AOD) using the formula: AOD = IOD/area [37].1 Antibodies: interleukin-10 (IL-10) (1:500, proteintech,

60269-1-Ig, China), Tumor Necrosis Factor-alpha (TNF-α) (1:300, proteintech, 60291-1-Ig, China), transforming growth factor-beta (TGF-β) (1:200, proteintech, 21898-1-AP, China), and vascular endothelial growth factor-A (VEGFA) (1:300, proteintech, 19003-1-AP, China).

2.10. Statistical analysis

The Statistical Package for Social Sciences 16.0 was used for the statistical analysis. Values were expressed as mean ± SEM. One-way analysis of variance was performed for comparisons between multiple groups. P < 0.05 was considered statistically significant.
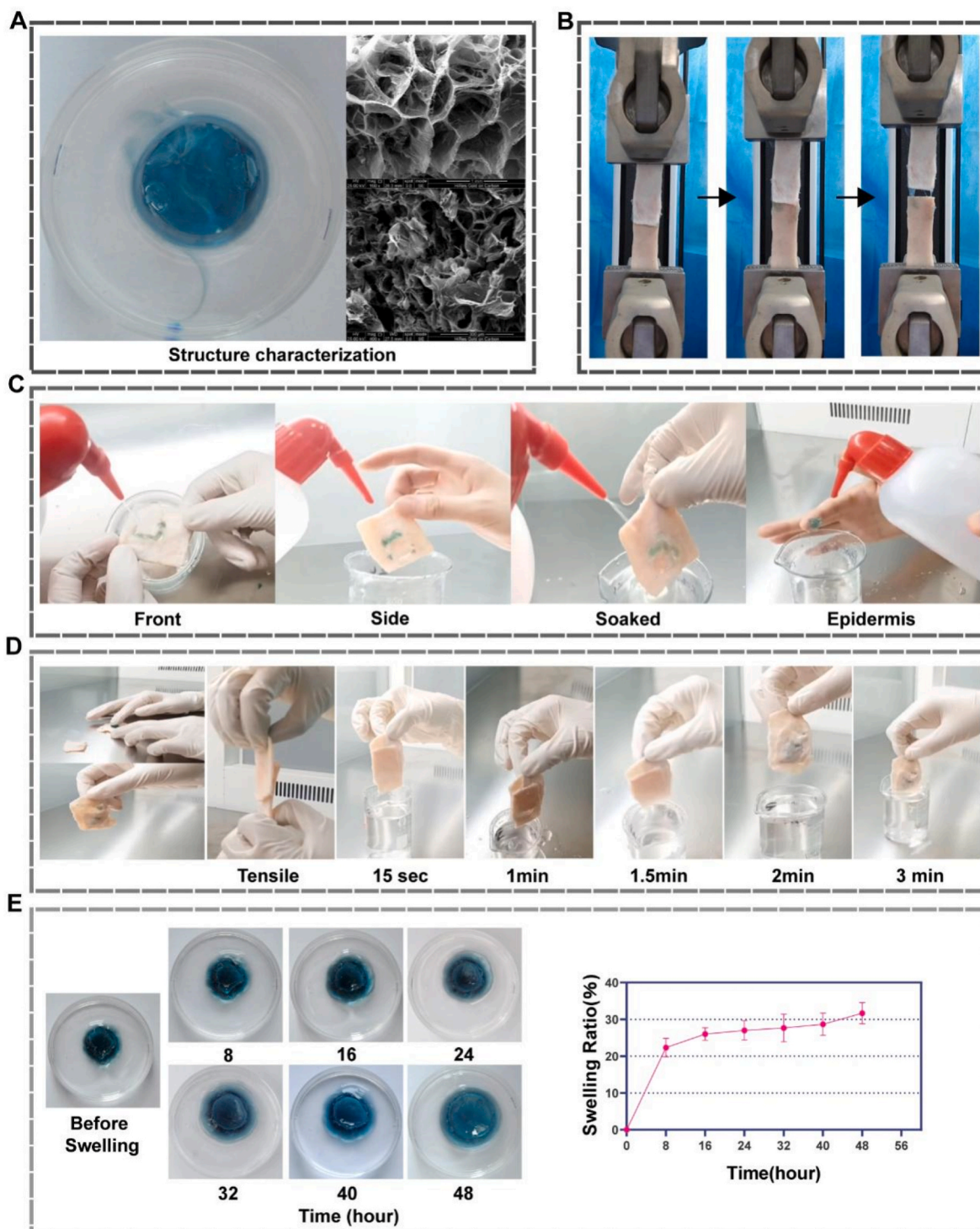

Fig. 2. Anti swelling, tensile performance and adhesion characterizations of the AS hydrogel. (A) Photo image and morphology of AS hydrogel. (B) Tensile property test. ((c) anti-flushing performance. (D) tensile resistance and (E) anti-swelling properties of AS hydrogel. All data are presented as mean ± standard deviation (n = 3).

3. Result and discussion

3.1. Morphology, adhesion, and swelling properties

A new biopolymer composite called AS hydrogel is made of CS and PVA and crosslinked using genipin. The two sequential steps that construct its dual network structure are as follows: first, genipin forms covalent bonds with the amino groups of CS; second, the hydroxyl groups of PVA establish hydrogen bonds with the remaining amino groups of CS, resulting in an interpenetrating network. Because of its dual network structure, AS hydrogel has better mechanical and biological qualities. Fig. 2A shows the photo image and SEM images of the hydrogel. The hydrogel had a light blue transparent color. Furthermore the SEM images showed that the pores of the hydrogel had greatly increase after being soaked in DI water for 1 h compared to that non-soaking condition.

It was shown that the nucleophilic reaction of genipin created covalent connections between the PVA and CS macromolecules, increasing the viscosity and stability of the hydrogel and facilitating its adequate adhesion to the tissue defect location. The AS hydroxyl or amino content of the hydrogel drops as genipin cross-links with CS, which lessens the adhesive properties of the hydrogel. This permits the hydrogel to passivate on its surface and inhibits unwanted adherence to other tissue surfaces, possibly leading to the hydrogel dislocating. Conversely, hydrogels that initially cling to the wound interface do so because of the persistence of certain hydrogen bonds, which means that additional genipin cross-linking does not break down their adherence. The optimal anti-adhesion substance sticks firmly to the injured peritoneal surface. We evaluated the adhesion strength of AS hydrogel using a biomechanical testing apparatus, through lapping between two segments of porcine skin tissue test. The findings demonstrated that AS hydrogel had an adhesion strength of 4.22 kPa (Fig. 2B). The adhesion performance of AS hydrogel was demonstrated in Fig. 3C when exposed to water. The hydrogel remained on the surface of pig skin, suggesting that the adhesion was adaptable to liquid flow settings. Furthermore, under stress tension (Fig. 2D), the AS hydrogel could continue exhibiting good adhesion performance in both air and water. The ability of the AS hydrogel to adhere to bodily application environments was shown by its adhesion property. Applying anti-swelling is essential as it acts as an anti-adhesion barrier. Genipin cross-linking decreases the free water content and pore size of the AS hydrogel network by increasing its density and hydrophobicity. This reduces the absorption and diffusion of water molecules in the hydrogel, which lowers the swelling behavior. After being immersed in PBS solution for 48 h, AS hydrogel had outstanding anti-swelling efficacy, as demonstrated by the swelling rate and photo images (Fig. 2E).

3.2. In vitro cytocompatibility and anti-inflammatory capacity of AS hydrogels

Novel biomaterials must have good biocompatibility and low cytotoxicity to be used in practice [38]. To evaluate the biocompatibility of AS hydrogel, we co-cultured HIEC-6, HK2 and SVHUC1 cells with it in this study. The Live and Dead Cell Double Staining assays, MTS and CCK8 assays and cytoskeletal fluorescence staining assays were used to carry out this study. As HK2 and SVHUC1 cells were co-cultured with the material for 72 h, there were no apparent abnormalities in their morphology as compared to the control group, as shown in Fig. 3A. After co-culturing HIEC-6 cells with the AS hydrogel for 72 h, the Live and Dead Cell Double Staining assays revealed results similar to the control group (Fig. 3B). The cells displayed good adhesion and extension patterns, clear nuclei, and no signs of cell senescence or apoptosis. Furthermore, the findings of MTS and CCK-8 showed that the cell proliferation in the material co-culture group was comparable to that of the blank control group, with the AS hydrogel group showing even more significant cell growth than the blank group (Fig. 3C–D). This improvement could be explained by the AS hydrogel material's ability to reduce pericellular inflammation. Inflammation following surgical
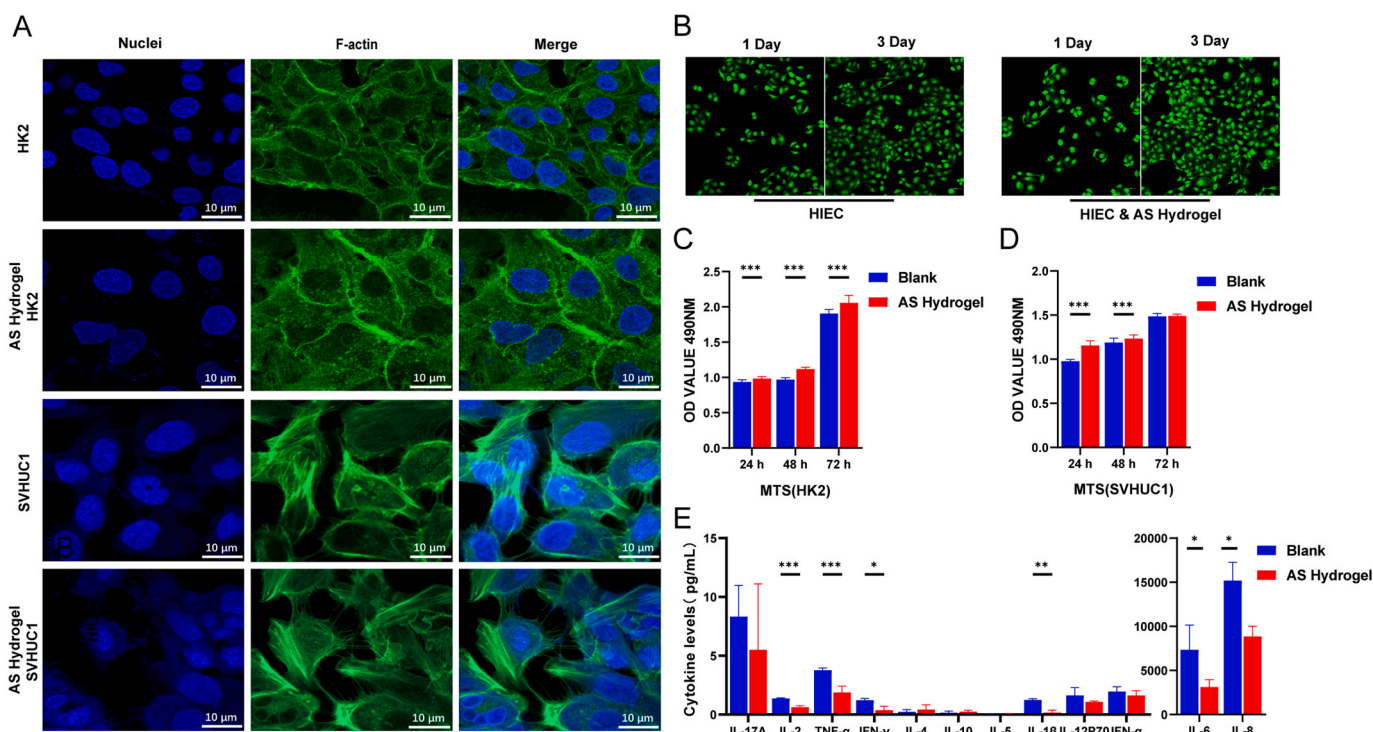

Fig. 3. The cytocompatibility and inflammatory cytokine levels of AS hydrogels. (A) Fluorescence microscopy images of HK2 and SVHUC1 cells (scale bars: 20 μm). (B) Live-Dead Staining Images of HIEC-6 Cells. (C–D) AS hydrogels, MTS, and cell counting kit-8 were used in co-cultured HK2 and SVHUC1 cells. (E) A comparison of the pro- and anti-inflammatory cytokine concentrations in HK2 and SVHUC1 cell supernatants following a 48-h co-culture with AS hydrogel. Error bars indicate ± standard deviation (n = 3), * and ** indicate P < 0.05 and P < 0.001, respectively.

trauma and damage frequently promotes the development of post-operative abdominal adhesions [39,40]. Therefore, effectively reducing inflammation is essential for avoiding these kinds of adhesions. After 48 h of co-culture, we analyzed the pro-inflammatory and anti-inflammatory factors in the cell supernatant, such as IL1β, IL2, IL4, IL5, IL6, IL8, IL17A, TNF-α, IFN-γ, IFN-α, and IL-12P70 to gauge the degree of inflammation [41]. The findings of the experiment showed that the cytosol of the AS hydrogel group had considerably lower levels of IL2, TNF-α, IFN-γ, IL6, and IL8 (P < 0.05) than the blank cell group (Fig. 3E). The cells in the AS hydrogel group showed fewer inflammatory reactions and were spared the adverse effects of inflammation. These findings were consistently mirrored by the expression levels of IL6 and IL8, which are more sensitive in the early inflammatory response. Adding AS hydrogel might have lessened inflammation around the cells, resulting in a more stable environment for cell proliferation.

3.3. In vivo evaluation of AS hydrogels on postoperative anti-adhesion

We performed studies utilizing an abdominal wall injury model and a rabbit cecum injury model to assess how well AS hydrogel prevented adhesions in the abdominal cavity. We used saline to rinse the control group's abdominal cavity and the injury site. We evenly administered the hydrogel to the abdominal wall damage and the cecum in the AS hydrogel group. The rabbits were put to death, and their bodies were dissected to look for adhesions between the cecum and the nearby intestinal or abdominal wall [42]. Fig. 1B shows the rabbit abdominal adhesion model, and the experimental stages detail the precise surgical technique.

We took tissue samples and pictures of the cecum and the abdomen wall at the suture lines 14 days post-surgery from each group. Then, we calculated the tissue adhesion score. Both at the site of damage and on the uninjured surfaces of the cecum and proximal mesentery, we could
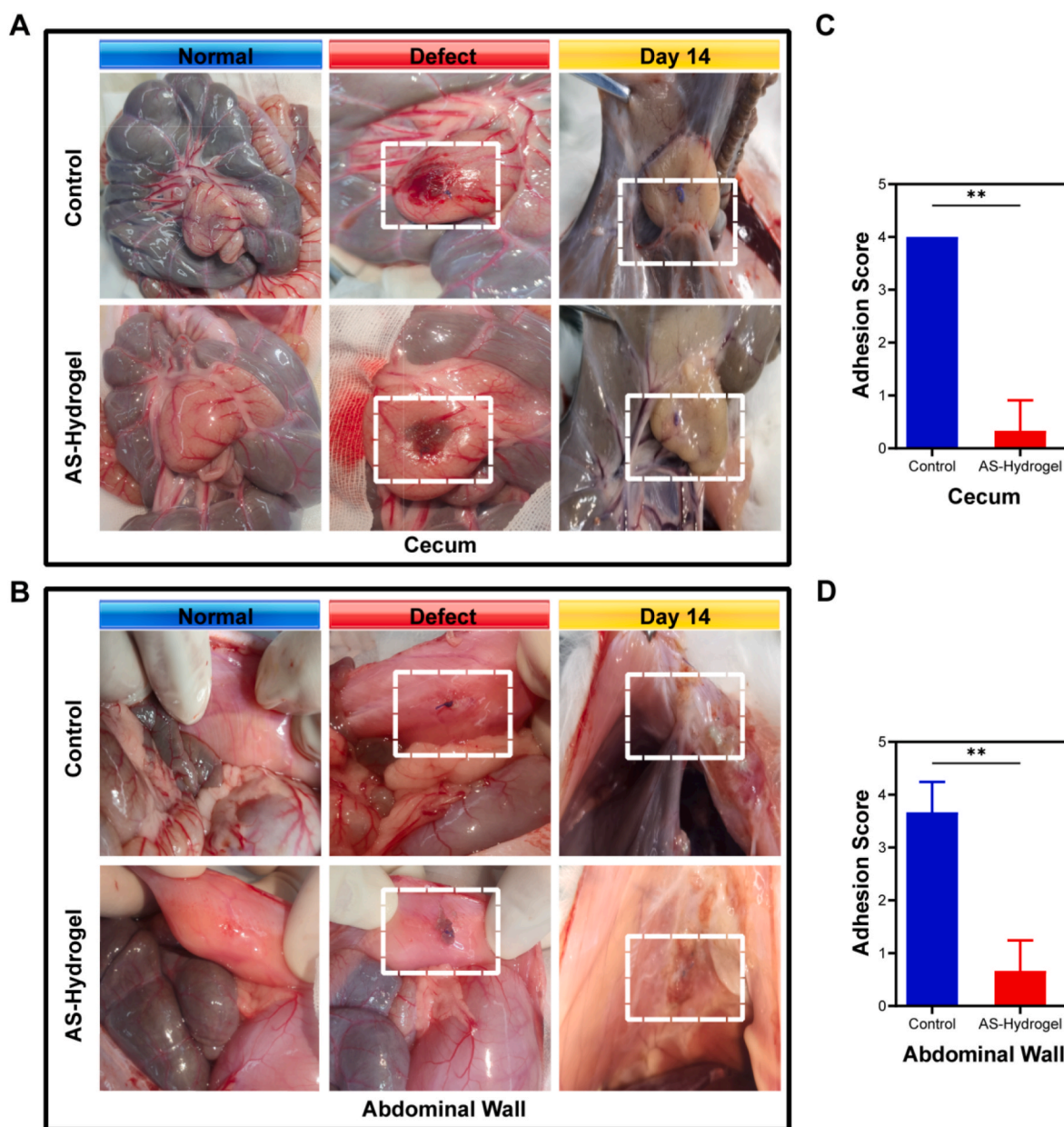

Fig. 4. Preventing abdominal adhesions after surgery in a large white rabbit model cecum and abdominal wall injuries. (A) A Great White rabbit cecum injury model with two distinct postoperative outcomes following untreated and covered AS hydrogel treatment. (B) Creating a model of an abdominal wall injury in a large white rabbit and observing two distinct postoperative results following administration of untreated and coated AS hydrogel. (C) Mean adhesion score of the abdominal wall (D), N = 3 independent samples for each group (control group, AS hydrogel group); error bars indicate ± SD, * and ** indicate P < 0.05 and P < 0.001, respectively.

see thick, vascularized adhesions in the control group (Fig. 4A). In the control group, all three instances exhibited score four adhesions [16]. On the other hand, the cecum trabeculae in the AS hydrogel group displayed either minimal or no adhesions; two cases had no adhesion, and one had a score of 1 adhesion. The flaws had been repaired almost entirely, with noticeable new capillaries at the healing locations, while the intestinal wall marks showed some rough scars. Since there was no hydrogel left behind, the healing process was successful. Significant adhesions to surrounding tissues were also seen at the abdominal wall markers in the control group, with two patients exhibiting a score of four adhesions and one case exhibiting a score of three adhesions (Fig. 4B). In contrast, the AS hydrogel group solely showed scar tissue. Fig. 4C and D shows that the mean score in the control group for the cecum abrasion model was four, and for the abdominal wall injury model was 3.66. By comparison, the AS hydrogel group scored considerably lower than the control group ($p < 0.001$), with scores for the cecum and belly wall of 0.33 and 0.66, respectively. These findings suggest that the AS hydrogel has outstanding qualities for accelerating wound healing and reducing adhesions following surgery. Notably, there was hardly any hydrogel left

on the surface of the injured abdominal wall and cecum, indicating the *in vivo* biodegradability of the AS hydrogel.

The histological features of intestinal and abdominal wall injuries were assessed using HE and Masson stains to illustrate further the AS hydrogel's *in vivo* anti-adhesion and anti-inflammatory properties [43, 44]. The submucosa and muscularis mucosae of the cecum were notably thicker, and the histological evaluation showed that the abraded portion of the gut wall had not fully healed in the control group. The connective tissue in the adhesion zone was jumbled and infected with lymphocytes, granulocytes, and macrophages. Furthermore, Fig. 5A showed a large concentration of neovascular endothelial cells. Sporadic necrotic myocytes were in the abdominal wall adhesion zone, but a large amount of collagen fiber hyperplasia gradually replaced these. The adhesion zone contained many lymphocytes, granulocytes, and vascular endothelial cells (Fig. 5B). According to these results, adhesion creation and inflammation are closely related, and the adhesion zone continuously proliferates when inflammation is repeatedly stimulated. The plasma membrane layer in the intestinal wall and the muscularis propria cells in the AS hydrogel group healed and rearranged correctly, leaving no
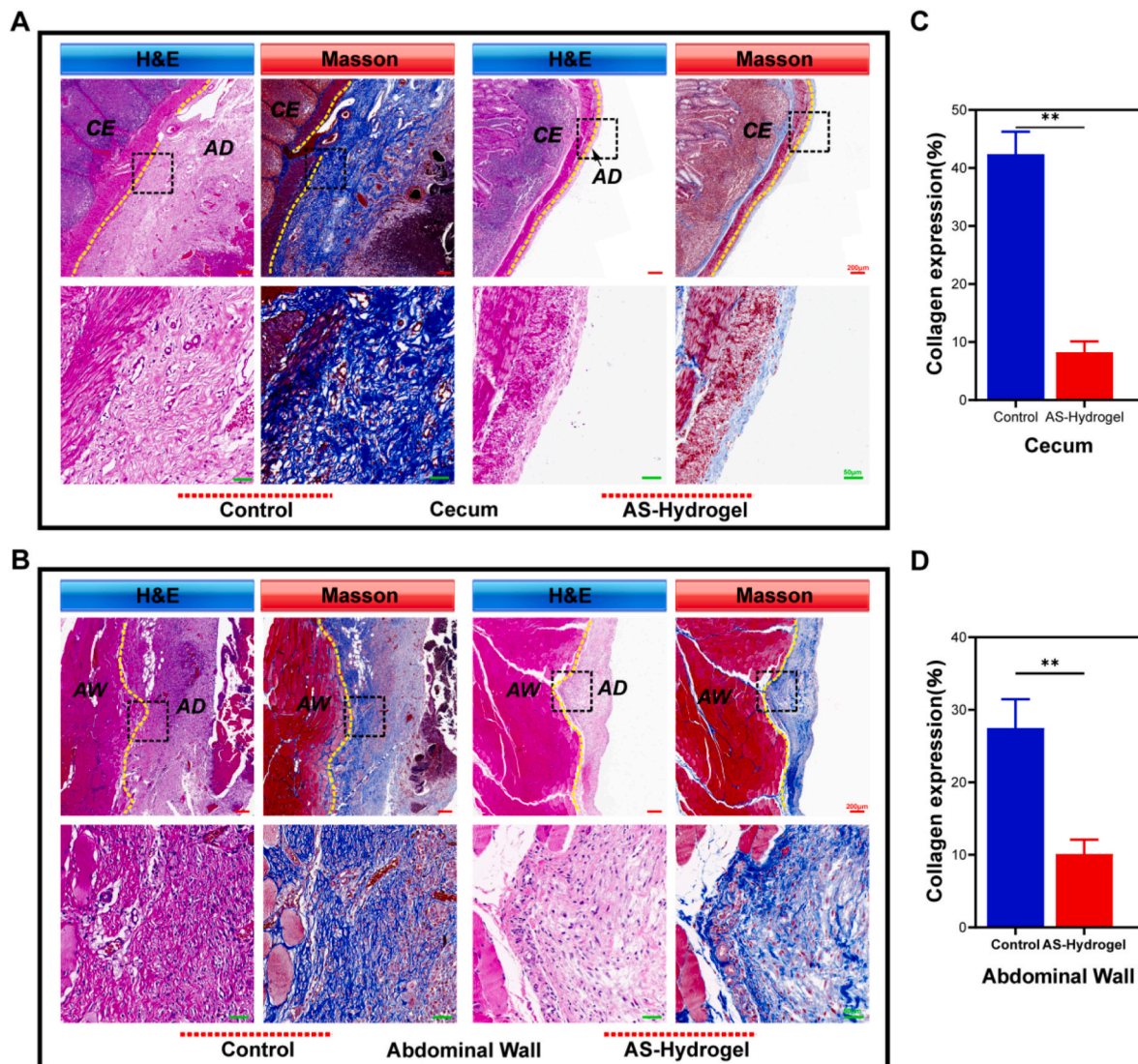

Fig. 5. Hematoxylin, eosin (H&E), and Masson trichrome staining were used to evaluate the adhesion model's cecum and abdominal wall. (A) Images of two tissue sections stained with H&E and Masson trichrome from the cecum location. Upper panel: scale bar, 200 μm; lower panel (enlarged view of the box above): scale bar, 50 μm. (B) Two sets of Masson trichrome and H&E-stained tissue section images of the abdominal wall region. Upper panel: scale bar, 200 μm; lower panel (enlarged view of the box above): scale bar, 50 μm. (C–D) Fibronectin expression statistical graphs in Masson findings. Error bars indicate ±SD, * and ** indicate $P < 0.05$ and $P < 0.001$, respectively. Ce: cecum, AW: abdominal wall, and AD: adhesion band.

hydrogel behind [45]. Only a small quantity of surrounding connective tissue was visible, and there was no discernible infiltration of inflammatory cells or fibrin growth. This illustrates the excellent anti-inflammatory properties of AS hydrogel even more. A new layer of mesothelial cells and a few loosely distributed collagen fibers were seen at the site of injury in the abdomen wall, along with a modest number of vascular endothelial cells. There was no visible hydrogel residue at the peritoneum. After this, Masson's findings demonstrated that the control group had a significant amount of misaligned dark blue collagen fiber deposition at the areas of abdominal wall abrasion and the cecum. However, at the cecum and abdominal wall abrasions, the AS hydrogel group only showed a small number of light blue, loosely distributed collagen fibers(Fig. 5A–B). Moreover, the hydrogel group showed a considerably reduced fibrin content in the abdomen wall and cecum compared to the control group (Fig. 5C–D). In conclusion, while the AS hydrogel group produced some fibrin, none stuck to nearby tissues. Furthermore, the AS hydrogel showed a robust anti-inflammatory effect that contrasted with the extensive inflammatory cell infiltration. The histological findings supported the results of adhesion scores, which also showed that AS hydrogel could successfully lower inflammatory responses and collagen deposition, resulting in the desired anti-adhesion effect.

3.4. In vivo evaluation of the anti-inflammatory capacity of AS hydrogels

It is primarily believed that activating and producing inflammatory cytokines, which trigger an inflammatory response, causes postoperative adhesions [46,47]. Our team has conducted in-depth pathology collection and immunohistochemistry investigations at the cecum and abdominal wall injury sites, focusing on this mechanism. Research has demonstrated that macrophages in these damaged tissues are proactive in generating endogenous inflammatory cytokines, including TNF-α [48,49]. TNF-α has several functions, including promoting the infiltration of inflammatory cells, promoting the development of fibrotic tissue and cellular apoptosis, and increasing adhesions by starting coagulation and fibrin layer formation [50–52]. In contrast, pro-inflammatory cytokines and fibrinogen-activating enzymes are downregulated by the anti-inflammatory cytokine IL-10, which promotes wound healing and inhibits the formation of adhesions [53,54]. Our experimental results show that in our established cecum and abdominal wall damage models, TNF-α expression was significantly reduced, whereas IL-10 expression was significantly elevated (Fig. 6A–B). These modifications are consistent with our immune factor dynamics in our co-culture system of cells and hydrogel.

Furthermore, our integrative pathological findings further revealed that TNF-α is widely expressed in the cytoplasm and nuclei of fibroblasts and vascular endothelial cells located within the wounded region of the intestinal wall in the control group [55,56]. On the other hand, an
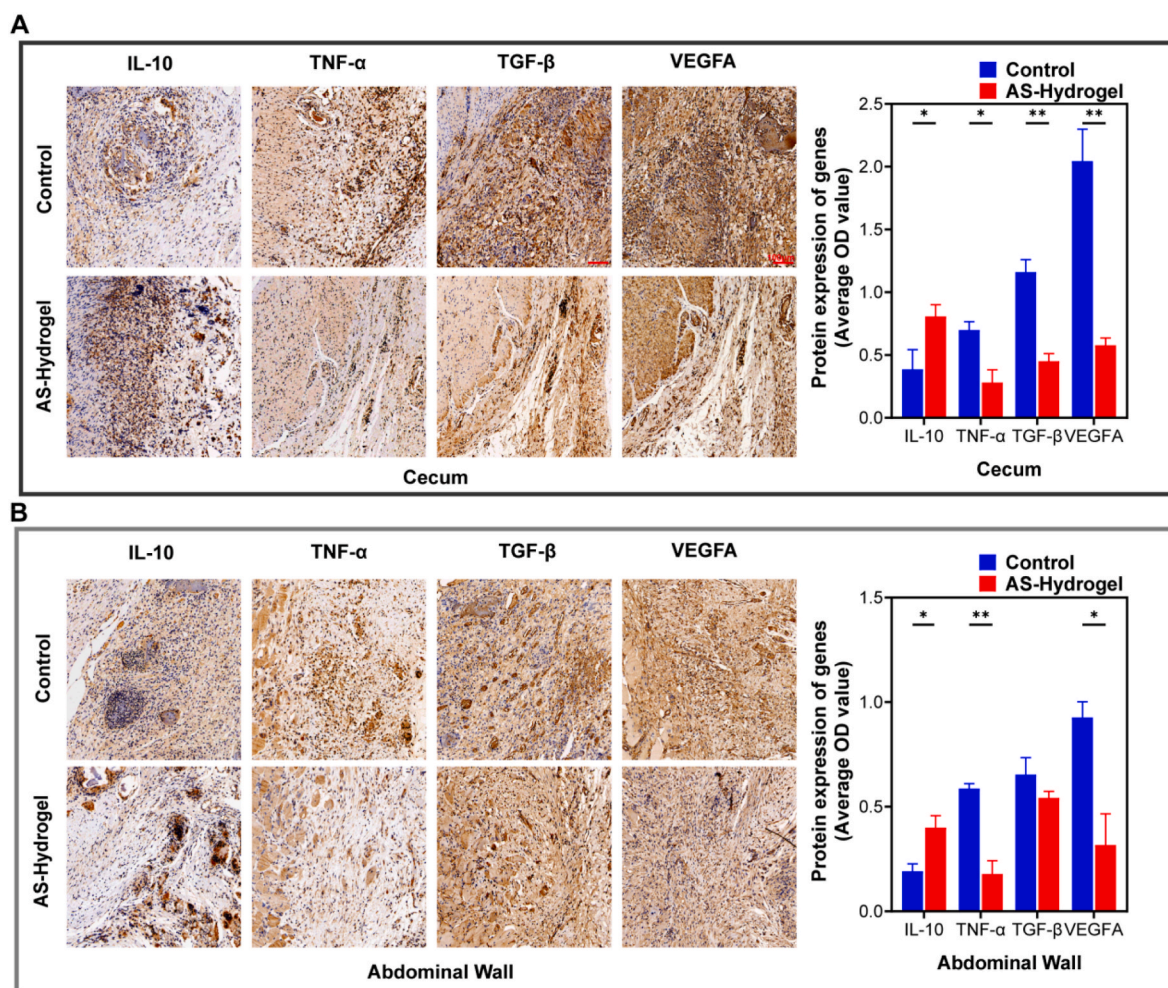

Fig. 6. Immunohistochemical staining images of inflammatory factors and vascular endothelial growth factor in the great white rabbit cecum and abdominal wall injury model. (A) Quantitative analysis of the immunohistochemistry results and immunostaining images (scale bar: 100 μm) of IL-10, TNF-α, IL-1β and VEGFA in the control and AS hydrogel treatment groups. (B) Quantitative analysis of the immunohistochemistry results and immunostaining images (scale bar: 100 μm) of IL-10, TNF-α, IL-1β and VEGFA in the control and AS hydrogel treatment groups. Error bars indicate ±SD, and * and ** indicate P < 0.05 and P < 0.001, respectively.

interesting limitation of TNF-α expression to negligible quantities in the connective tissue and vascular endothelial cells was detected following the application of anti-inflammatory AS hydrogel, suggesting a noticeable relief of inflammation [57]. Moreover, IL-10 showed a broad distribution pattern across mesenchymal cells, inflammatory cells, fibroblasts and calcifications in the intestinal wall and adhesive regions. Its expression became noticeably more prominent after the AS hydrogel treatment. Notably, our study also emphasizes that fibrogenic cytokine TGF-β and VEGFA play a role in this process. TGF-β, in its active state, significantly increases the extracellular matrix component secretion, ultimately leading to adhesion development. To enhance fibrin deposition and fibrosis, which leads to increased abdominal adhesions, VEGFA enhances this process by stimulating angiogenesis and vascular endothelial cell proliferation. In line with previous research findings, we further demonstrate that decreased VEGFA expression causes peritoneal adhesions to be effectively downregulated in mice following surgery. To be more precise, in our well-established model of cecal injury, TGF-β and VEGFA were much lower than in the control group (Fig. 6A). TGF-β expression showed a slight decrease in the abdominal wall damage model, although VEGFA expression in the model was similar to that of the control group (Fig. 6B). All of these findings supported the remarkable anti-inflammatory effect of AS hydrogel in all of the injury models that have been studied.

4. Conclusion

In conclusion, a unique type of CS-PVA composite hydrogel was created, and the resulting AS hydrogel has excellent tissue adhesion and anti-swelling properties. AS hydrogel was found to have good biocompatibility and to significantly lower the level of inflammation around cells, according to the evaluation of cells. Furthermore, in a rabbit model with cecum and abdominal wall injuries, the AS hydrogel showed superior prevention of intraperitoneal adhesion. These findings showed that AS hydrogel's excellent anti-inflammatory and biodegradability can effectively prevent the adhesion of the injured intestinal and abdominal walls during surgery. AS hydrogel is the ideal material to prevent postoperative abdominal adhesion.

CRediT authorship contribution statement

Yiqiao Huang: Writing - original draft. **Jiefang Zheng:** Methodology. **Guohao Zeng:** Data curation. **Huanhuan Xu:** Methodology. **Yangyang Lv:** Investigation. **Xue Liang:** Data curation. **Lin Jin:** Project administration, Writing - review & editing. **Xianhan Jiang:** Funding acquisition, Project administration, Writing - review & editing.

Declaration of competing interest

The authors declare that they have no known competing financial interests or personal relationships that could have appeared to influence the work reported in this paper.

Data availability

Data will be made available on request.

Acknowledgments

References

[1] X. Zhang, G. Chen, Y. Wang, L. Fan, Y. Zhao, Arrowhead composite microneedle Patches with anisotropic surface adhesion for preventing intrauterine adhesions, Adv. Sci. 9 (2022), e2104883.

[2] S.M. Mayes, J. Davis, J. Scott, V. Aguilar, S.A. Zawko, S. Swinnea, D.L. Peterson, J. G. Hardy, C.E. Schmidt, Polysaccharide-based films for the prevention of unwanted postoperative adhesions at biological interfaces, Acta Biomater. 106 (2020) 92–101.

[3] D. Jin, S. Yang, S. Wu, M. Yin, H. Kuang, A functional PVA aerogel-based membrane obtaining sutureability through modified electrospinning technology and achieving promising anti-adhesion effect after cardiac surgery, Bioact. Mater. 10 (2022) 355–366.

[4] J. Gao, J. Wen, D. Hu, K. Liu, Y. Zhang, X. Zhao, K. Wang, Bottlebrush inspired injectable hydrogel for rapid prevention of postoperative and recurrent adhesion, Bioact. Mater. 16 (2022) 27–46.

[5] J. Tang, Z. Xiang, M.T. Bernards, S. Chen, Peritoneal adhesions: occurrence, prevention and experimental models, Acta Biomater. 116 (2020) 84–104.

[6] R.L. De Wilde, R. Devassy, R. Broek, C.E. Miller, A. Adlan, P. Aquino, S. Becker, F. Darmawan, M. Gergolet, M. Habana, C.K. Khoo, P.R. Koninckx, M. Korell, H. Krentel, O. Musigavong, G. Pistofidis, S. Puntambekar, I.A. Rachman, F. Sendag, M. Wallwiener, L.R.L. Torres-de, The future of adhesion prophylaxis trials in abdominal surgery: an expert global consensus, J. Clin. Med. 11 (2022).

[7] Q. Hu, X. Xia, Z. Kang, P. Song, Z. Liu, M. Wang, X. Lu, W. Guan, S. Liu, A review of physiological and cellular mechanisms underlying fibrotic postoperative adhesion, Int. J. Biol. Sci. 17 (2021) 298–306.

[8] T. Ito, Y. Shintani, L. Fields, M. Shiraishi, M.N. Podaru, S. Kainuma, K. Yamashita, K. Kobayashi, M. Perretti, F. Lewis-McDougall, K. Suzuki, Cell barrier function of resident peritoneal macrophages in postoperative adhesions, Nat. Commun. 12 (2021) 2232.

[9] I.H. Yang, Y.S. Chen, J.J. Li, Y.J. Liang, T.C. Lin, S. Jakfar, M. Thacker, S.C. Wu, F. H. Lin, The development of laminin-alginate microspheres encapsulated with Ginsenoside Rg1 and ADSCs for breast reconstruction after lumpectomy, Bioact. Mater. 6 (2021) 1699–1710.

[10] E. Zhang, J. Yang, K. Wang, B. Song, H. Zhu, X. Han, Y. Shi, C. Yang, Z. Zeng, Z. Cao, Biodegradable zwitterionic cream gel for effective prevention of postoperative adhesion, Adv. Funct. Mater. 31 (2021).

[11] X. Zhao, X. Piao, B. Liu, R. Xie, T. Zhan, M. Liang, J. Tian, R. Wang, C. Chen, J. Zhu, Y. Zhang, B. Yang, NFK prevent postoperative abdominal adhesion through downregulating the TGF-beta1 signaling pathway, Mol. Biol. Rep. 50 (2023) 279–288.

[12] S.N. Carmichael, J. Shin, J.W. Vaughan, P.K. Chandra, J.B. Holcomb, A.J. Atala, Regenerative medicine therapies for prevention of abdominal adhesions: a scoping review, J. Surg. Res. 275 (2022) 252–264.

[13] Z. Wan, J. He, Y. Yang, T. Chong, J. Wang, B. Guo, L. Xue, Injectable adhesive self-healing biocompatible hydrogel for haemostasis, wound healing, and postoperative tissue adhesion prevention in nephron-sparing surgery, Acta Biomater. 152 (2022) 157–170.

[14] E. Zhang, J. Yang, K. Wang, B. Song, H. Zhu, X. Han, Y. Shi, C. Yang, Z. Zeng, Z. Cao, Biodegradable zwitterionic cream gel for effective prevention of postoperative adhesion, Adv. Funct. Mater. 31 (2021).

[15] E. Zhang, B. Song, Y. Shi, H. Zhu, X. Han, H. Du, C. Yang, Z. Cao, Fouling-resistant zwitterionic polymers for complete prevention of postoperative adhesion, P. Natl. Acad. Sci. USA. 117 (2020) 32046–32055.

[16] E. Zhang, Q. Guo, F. Ji, X. Tian, J. Cui, Y. Song, H. Sun, J. Li, F. Yao, Thermoresponsive polysaccharide-based composite hydrogel with antibacterial and healing-promoting activities for preventing recurrent adhesion after adhesiolysis, Acta Biomater. 74 (2018) 439–453.

[17] J.H. Yang, C.D. Chen, S.U. Chen, Y.S. Yang, M.J. Chen, The influence of the location and extent of intrauterine adhesions on recurrence after hysteroscopic adhesiolysis, BJOG An Int. J. Obstet. Gynaecol. 123 (2016) 618–623.

[18] J. Gao, J. Wen, D. Hu, K. Liu, Y. Zhang, X. Zhao, K. Wang, Bottlebrush inspired injectable hydrogel for rapid prevention of postoperative and recurrent adhesion, Bioact. Mater. 16 (2022) 27–46.

[19] J. Gao, J. Wen, D. Hu, K. Liu, Y. Zhang, X. Zhao, K. Wang, Bottlebrush inspired injectable hydrogel for rapid prevention of postoperative and recurrent adhesion, Bioact. Mater. 16 (2022) 27–46.

[20] E. Zhang, J. Yang, K. Wang, B. Song, H. Zhu, X. Han, Y. Shi, C. Yang, Z. Zeng, Z. Cao, Biodegradable zwitterionic cream gel for effective prevention of postoperative adhesion, Adv. Funct. Mater. 31 (2021).

[21] E. Zhang, J. Yang, K. Wang, B. Song, H. Zhu, X. Han, Y. Shi, C. Yang, Z. Zeng, Z. Cao, Biodegradable zwitterionic cream gel for effective prevention of postoperative adhesion, Adv. Funct. Mater. 31 (2021).

[22] L. Li, N. Wang, X. Jin, R. Deng, S. Nie, L. Sun, Q. Wu, Y. Wei, C. Gong, Biodegradable and injectable in situ cross-linking chitosan-hyaluronic acid based hydrogels for postoperative adhesion prevention, Biomaterials 35 (2014) 3903–3917.

[23] J. Li, W. Xu, J. Chen, D. Li, K. Zhang, T. Liu, J. Ding, X. Chen, Highly bioadhesive polymer membrane continuously releases cytostatic and anti-inflammatory drugs for peritoneal adhesion prevention, ACS Biomater. Sci. Eng. 4 (2018) 2026–2036.

[24] L.M. Stapleton, A.N. Steele, H. Wang, H.H. Lopez, A.C. Yu, M.J. Paulsen, A. Smith, G.A. Roth, A.D. Thakore, H.J. Lucian, K.P. Totherow, S.W. Baker, Y. Tada, J. M. Farry, A. Eskandari, C.E. Hironaka, K.J. Jaatinen, K.M. Williams, H. Bergamasco, C. Marschel, B. Chadwick, F. Grady, M. Ma, E.A. Appel, Y.J. Woo, Use of a supramolecular polymeric hydrogel as an effective postoperative pericardial adhesion barrier, Nat. Biomed. Eng. 3 (2019) 611–620.

[25] Y. Huang, R. Shi, M. Gong, J. Zhang, W. Li, Q. Song, C. Wu, W. Tian, Icariin-loaded electrospun PCL/gelatin sub-microfiber mat for preventing epidural adhesions after laminectomy, Int. J. Nanomed. 13 (2018) 4831–4844.

[26] J. Gao, J. Wen, D. Hu, K. Liu, Y. Zhang, X. Zhao, K. Wang, Bottlebrush inspired injectable hydrogel for rapid prevention of postoperative and recurrent adhesion, Bioact. Mater. 16 (2022) 27–46.

[27] M. Bacakova, J. Musilkova, T. Riedel, D. Stranska, E. Brynda, M. Zaloudkova, L. Bacakova, The potential applications of fibrin-coated electrospun polylactide nanofibers in skin tissue engineering, Int. J. Nanomed. 11 (2016) 771–789.

[28] S. Dhall, T. Coksaygan, T. Hoffman, M. Moorman, A. Lerch, J.Q. Kuang, M. Sathyamoorthy, A. Danilkovitch, Viable cryopreserved umbilical tissue (vCUT) reduces postoperative adhesions in a rabbit abdominal adhesion model, Bioact. Mater. 4 (2019) 97–106.

[29] H. Wang, X. Yi, T. Liu, J. Liu, Q. Wu, Y. Ding, Z. Liu, Q. Wang, An integrally formed janus hydrogel for robust wet-tissue adhesive and anti-postoperative adhesion, Adv. Mater. 35 (2023), e2300394.

[30] Z. Wan, J. He, Y. Yang, T. Chong, J. Wang, B. Guo, L. Xue, Injectable adhesive self-healing biocompatible hydrogel for haemostasis, wound healing, and postoperative tissue adhesion prevention in nephron-sparing surgery, Acta Biomater. 152 (2022) 157–170.

[31] Y. Wang, Y. Xu, W. Zhai, Z. Zhang, Y. Liu, S. Cheng, H. Zhang, In-situ growth of robust superlubricated nano-skin on electrospun nanofibers for postoperative adhesion prevention, Nat. Commun. 13 (2022) 5056.

[32] J. Ke, M. Chen, S. Ma, L. Zhang, L. Zhang, Circular RNA VMA21 ameliorates lung injury in septic rat via targeting microRNA-497-5p/CD2-associated protein axis, Bioengineered 13 (2022) 5453–5466.

[33] E. Zhang, Q. Guo, F. Ji, X. Tian, J. Cui, Y. Song, H. Sun, J. Li, F. Yao, Thermoresponsive polysaccharide-based composite hydrogel with antibacterial and healing-promoting activities for preventing recurrent adhesion after adhesiolysis, Acta Biomater. 74 (2018) 439–453.

[34] J. Gao, J. Wen, D. Hu, K. Liu, Y. Zhang, X. Zhao, K. Wang, Bottlebrush inspired injectable hydrogel for rapid prevention of postoperative and recurrent adhesion, Bioact. Mater. 16 (2022) 27–46.

[35] H. Liu, Q. Pang, F. Cao, Z. Liu, W. Wei, Z. Li, Q. Long, Y. Jiao, Number 2 feibi recipe ameliorates pulmonary fibrosis by inducing autophagy through the GSK-3beta/mTOR pathway, Front. Pharmacol. 13 (2022), 921209.

[36] M. Mehdizadeh, H. Weng, D. Gyawali, L. Tang, J. Yang, Injectable citrate-based mussel-inspired tissue bioadhesives with high wet strength for sutureless wound closure, Biomaterials 33 (2012) 7972–7983.

[37] C. Wang, R. Peng, M. Zeng, Z. Zhang, S. Liu, D. Jiang, Y. Lu, F. Zou, An autoregulatory feedback loop of miR-21/VMP1 is responsible for the abnormal expression of miR-21 in colorectal cancer cells, Cell Death Dis. 11 (2020) 1067.

[38] B. Yi, T. Wu, N. Zhu, Y. Huang, X. Yang, L. Yuan, Y. Wu, X. Liang, X. Jiang, The clinical significance of CTC enrichment by GPC3-IML and its genetic analysis in hepatocellular carcinoma, J. Nanobiotechnol. 19 (2021) 74.

[39] Y. Wu, G. Wei, J. Yu, Z. Chen, Z. Xu, R. Shen, T. Liang, L. Zheng, K. Wang, X. Sun, X. Li, Danhong injection alleviates postoperative intra-abdominal adhesion in a rat model, Oxid. Med. Cell. Longev. 2019 (2019), 4591384.

[40] J. Barambio, M. Garcia-Arranz, C.P. Villarejo, P.J. Velez, L.V. Clemente, S. G. Gomez-Heras, H. Guadalajara, D. Garcia-Olmo, Chemical scalpel: an experimental collagenase-based treatment for peritoneal adhesions, Biology-Basel 11 (2022).

[41] C. Lenoir, Y. Daali, V. Rollason, F. Curtin, Y. Gloor, M. Bosilkovska, B. Walder, C. Gabay, M.J. Nissen, J.A. Desmeules, D. Hannouche, C.F. Samer, Impact of acute inflammation on cytochromes p450 activity assessed by the geneva cocktail, Clin. Pharmacol. Ther. 109 (2021) 1668–1676.

[42] S.M. Mayes, J. Davis, J. Scott, V. Aguilar, S.A. Zawko, S. Swinnea, D.L. Peterson, J. G. Hardy, C.E. Schmidt, Polysaccharide-based films for the prevention of unwanted postoperative adhesions at biological interfaces, Acta Biomater. 106 (2020) 92–101.

[43] A. Stasi, R. Franzin, C. Divella, F. Sallustio, C. Curci, A. Picerno, P. Pontrelli, F. Staffieri, L. Lacitignola, A. Crovace, V. Cantaluppi, D. Medica, C. Ronco, M. de Cal, A. Lorenzin, M. Zanella, G.B. Pertosa, G. Stallone, L. Gesualdo, G. Castellano, PMMA-based continuous hemofiltration modulated complement activation and renal dysfunction in lps-induced acute kidney injury, Front. Immunol. 12 (2021), 605212.

[44] F.Z. Xin, Z.H. Zhao, X.L. Liu, Q. Pan, Z.X. Wang, L. Zeng, Q.R. Zhang, L. Ye, M. Y. Wang, R.N. Zhang, Z.Z. Gong, L.J. Huang, C. Sun, F. Shen, L. Jiang, J.G. Fan, Escherichia fergusonii promotes nonobese nonalcoholic fatty liver disease by interfering with host hepatic lipid metabolism through its own msRNA 23487, Cell Mol. Gastroenter. 13 (2022) 827–841.

[45] S. Barbon, E. Stocco, D. Dalzoppo, S. Todros, A. Canale, R. Boscolo-Berto, P. Pavan, V. Macchi, C. Grandi, R. De Caro, A. Porzionato, Halogen-mediated partial oxidation of polyvinyl alcohol for tissue engineering purposes, Int. J. Mol. Sci. 21 (2020).

[46] Y. Wu, G. Wei, J. Yu, Z. Chen, Z. Xu, R. Shen, T. Liang, L. Zheng, K. Wang, X. Sun, X. Li, Danhong injection alleviates postoperative intra-abdominal adhesion in a rat model, Oxid. Med. Cell. Longev. 2019 (2019), 4591384.

[47] X. Ding, X. Yu, C. Yang, D. Wu, Y. Zhao, Multifunctional go hybrid hydrogel scaffolds for wound healing, Res. Chi. 2022 (2022), 9850743.

[48] B. Shen, C. Zhao, Y. Wang, Y. Peng, J. Cheng, Z. Li, L. Wu, M. Jin, H. Feng, Aucubin inhibited lipid accumulation and oxidative stress via Nrf2/HO-1 and AMPK signalling pathways, J. Cell Mol. Med. 23 (2019) 4063–4075.

[49] Z. Lu, L. Feng, W.D. Jiang, P. Wu, Y. Liu, J. Jiang, S.Y. Kuang, L. Tang, S.W. Li, X. A. Liu, C.B. Zhong, X.Q. Zhou, Mannan oligosaccharides application: multipath restriction from aeromonas hydrophila infection in the skin barrier of grass carp (ctenopharyngodon idella), Front. Immunol. 12 (2021), 742107.

[50] S. Wang, Y. Li, W. Li, K. Zhang, Z. Yuan, Y. Cai, K. Xu, J. Zhou, Z. Du, Curcuma oil ameliorates benign prostatic hyperplasia through suppression of the nuclear factor-kappa B signaling pathway in rats, J. Ethnopharmacol. 279 (2021) 113703.

[51] J. Hao, B. Li, H.Q. Duan, C.X. Zhao, Y. Zhang, C. Sun, B. Pan, C. Liu, X.H. Kong, X. Yao, S.Q. Feng, Mechanisms underlying the promotion of functional recovery by deferoxamine after spinal cord injury in rats, Neural. Regen. Res. 12 (2017) 959–968.

[52] X. Chen, X. Zhao, H. Wang, Z. Yang, J. Li, H. Suo, Prevent effects of lactobacillus fermentum hy01 on dextran sulfate sodium-induced colitis in mice, Nutrients 9 (2017).

[53] L.L. Zou, J.R. Li, H. Li, J.L. Tan, M.X. Wang, N.N. Liu, R.M. Gao, H.Y. Yan, X. K. Wang, B. Dong, Y.H. Li, Z.G. Peng, TGF-beta isoforms inhibit hepatitis C virus propagation in transforming growth factor beta/SMAD protein signalling pathway dependent and independent manners, J. Cell Mol. Med. 25 (2021) 3498–3510.

[54] C. Zhu, S. Han, X. Zeng, C. Zhu, Y. Pu, Y. Sun, Multifunctional thermo-sensitive hydrogel for modulating the microenvironment in Osteoarthritis by polarizing macrophages and scavenging ROS, J. Nanobiotechnol. 20 (2022) 221.

[55] B. Ghadrdoost, A.A. Vafaei, A. Rashidy-Pour, R. Hajisoltani, A.R. Bandegi, F. Motamedi, S. Haghighi, H.R. Sameni, S. Pahlvan, Protective effects of saffron extract and its active constituent crocin against oxidative stress and spatial learning and memory deficits induced by chronic stress in rats, Eur. J. Pharmacol. 667 (2011) 222–229.

[56] S. Samarghandian, M. Azimi-Nezhad, T. Farkhondeh, Immunomodulatory and antioxidant effects of saffron aqueous extract (Crocus sativus L.) on streptozotocin-induced diabetes in rats, Indian Heart J. 69 (2017) 151–159.

[57] O. Simonetti, G. Lucarini, G. Morroni, F. Orlando, R. Lazzarini, A. Zizzi, L. Brescini, M. Provinciali, A. Giacometti, A. Offidani, O. Cirioni, New evidence and insights on dalbavancin and wound healing in a mouse model of skin infection, Antimicrob. Agents Chemother. 64 (2020).